Inorg. Chem. **2003**, *42*, 4632–4639

A New Dinuclear Ti(IV)–Peroxo–Citrate Complex from Aqueous Solutions. Synthetic, Structural, and Spectroscopic Studies in Relevance to Aqueous Titanium(IV)–Peroxo–Citrate Speciation

M. Dakanali,[†] E. T. Kefalas,[†] C. P. Raptopoulou,[‡] A. Terzis,[‡] G. Voyiatzis,[||] I. Kyrikou,[§] T. Mavromoustakos,[§] and A. Salifoglou*,[†]

Department of Chemistry, University of Crete, Heraklion 71409, Greece, Institute of Materials Science, NCSR "Demokritos", Aghia Paraskevi 15310, Attiki, Greece, National Hellenic Research Foundation, Institute of Organic and Pharmaceutical Chemistry, Athens 11635, Greece, and Foundation for Research and Technology Hellas (FORTH), Institute of Chemical Engineering and High Temperature Chemical Processes (ICE/HT), Patras 26500, Greece

Received March 20, 2003

The wide use of titanium in applied materials has prompted pertinent studies targeting the requisite chemistry of that metal's biological interactions. In order to understand such interactions as well as the requisite titanium aqueous speciation, we launched investigations on the synthesis and spectroscopic and structural characterization of Ti(IV) species with the physiological citric acid. Aqueous reactions of $TiCl_4$ with citric acid in the presence of H_2O_2 and neutralizing ammonia afforded expediently the red crystalline material $(NH_4)_4[Ti_2(O_2)_2(C_6H_4O_7)_2]\cdot 2H_2O$ (**1**). Complex **1** was further characterized by UV–vis, FT-IR, FT- and laser-Raman, NMR, and finally by X-ray crystallography. Compound **1** crystallizes in the monoclinic space group $P2_1/n$, with $a = 10.360(4)$ Å, $b = 10.226(4)$ Å, $c = 11.478(6)$ Å, $\beta = 107.99(2)^\circ$, $V = 1156.6(9)$ Å^3, and $Z = 2$. The X-ray structure of **1** reveals a dinuclear anionic complex containing a $Ti^{IV}_2O_2$ core. In that central unit, two fully deprotonated citrate ligands are coordinated to the metal ions through their carboxylate moieties in a monodentate fashion. The central alkoxides serve as bridges to the two titanium ions. Also attached to the $Ti^{IV}_2O_2$ core are two peroxo ligands each bound in a side-on fashion to the respective metal ions. NH_4^+ ions neutralize the 4– charge of the anion in **1**, further contributing to the stability of the derived lattice through H-bond formation. The structural similarities and differences with congener vanadium(V)–peroxo–citrate complexes may point out potential implications in the chemistry of titanium with physiological ligands, when the former is present in a biologically relevant medium.

Introduction

Titanium is an early transition metal, which has found numerous applications.[1] In the form of Ti(III)−citrate, it has been used extensively in recent years to probe redox reactions involving enzyme catalytic functions (i.e., nitrogenase enzyme components), thus facilitating understanding of mechanism(s) involved in metallobiological processes (i.e., nitrogen fixation).[2] Moreover, titanium regularly constitutes an essential component of alloys and composites used in prosthetic materials destined for orthopedic surgical rectifications in humans,[3] dental implants and fillings,[4] and others.[5] In all of the aforementioned applications, titanium comes in

* To whom correspondence should be addressed. Phone: +30-2810-393-652. Fax: +30-2810-393-601. E-mail: salif@chemistry.uoc.gr.
[†] University of Crete.
[‡] Institute of Materials Science, NCSR "Demokritos".
[§] National Hellenic Research Foundation,.
[||] Foundation for Research and Technology Hellas (FORTH).

(1) (a) Biehl, V.; Wack, T.; Winter, S.; Seyfert, U. T.; Breme, J. *Biomol. Eng.* **2002**, *19*, 97−101. (b) Thull, R. *Biomol. Eng.* **2002**, *19*, 43−50. (c) Paladino, J.; Stimac, D.; Rotim, K.; Pirker, N.; Stimac, A. *Minim. Invasive Neurosurg.* **2000**, *43*, 72−74. (d) Sumi, Y.; Hattori, H.; Hayashi, K.; Ueda, M. *J. Endodon.* **1997**, *23*, 121−123. (e) Yuan, Y.; Li, X.; Sun, J.; Ding, K. *J. Am. Chem. Soc.* **2002**, *124*, 14866−14867. (f) Kii, S.; Maruoka, K. *Chirality* **2003**, *15*, 68−70.

(2) Schneider, K.; Müller, A.; Krahn, E.; Hagen, W. R.; Wassink, H.; Knüttel, K.-H. *Eur. J. Biochem.* **1995**, *230*, 666−675.

(3) Bardos, D. In *Titanium and Zirconium Alloys in Orthopedic Applications*; Altobelli, D. E., Gresser, J. D., Schwartz, E. R., Trantolo, D. J., Wise, D. L., Yaszemski, M. J., Eds.; Encyclopedic Handbook of Biomaterials and Bioengineering; Marcel Dekker: New York, 1995; 509−548.

(4) (a) Degidi, M.; Petrone, G.; Iezzi, G.; Piattelli, A. *Clin. Implant. Dent. Relat. Res.* **2002**, *4*, 110−114. (b) Knabe, C.; Klar, F.; Fitzner, R.; Radlanski, R. J.; Gross, U. *Biomaterials* **2002**, *23*, 3235−3245.

10.1021/ic0343051 CCC: $25.00
Published on Web 07/01/2003

contact with biological tissues, thus giving rise to interactions with a host of biomolecules. Both high molecular mass and low molecular mass ligands have the potential to interact with titanium, gradually inducing its solubilization. In the course of this process, metal ion−ligand interactions develop, which result in the formation of soluble titanium−ligand complexes. The latter could have the potential to further interact with cellular components in the intracellular or extracellular matrix, thereby raising the possibility of a symptomatic response from the host organism. Such interactions could, in principle, emerge at both the protein and nucleic acid level, concomitantly affording toxic and/or nontoxic effects. To this end, a number of studies have been conducted that target the consequences of titanium interactions with physiological components at the cellular level.[6] All of these studies were launched with the aim of understanding the nature of titanium−biological tissue interactions, as the latter may reflect possible consequences of the titanium metal coming in contact with human tissue as a component of prosthetic materials.[7]

In biological interactions of titanium with low molecular mass ligands, the nature and oxidation state of titanium in the arising complex species are of importance. To this end, the aqueous speciation of titanium in its prominent oxidation states Ti(III) and Ti(IV) with physiological ligands is of essence. On this basis, a better understanding of the possible role(s) of the metal in biology could be deduced. Among the target ligands with which Ti(IV) or Ti(III) could chemically interact is citric acid. As a physiological molecule, citric acid is abundant in human plasma (∼0.1 mM).[8] As a tricarboxylic acid, citric acid possesses the chemical and structural attributes required for the promotion of aqueous chemistries with metal ions such as titanium. Knowledge of such chemistries, however, is presently very limited, with a representative example being the $(NH_4)_8[Ti_4(C_6H_4O_7)_4(O_2)_4]\cdot 8H_2O$ complex.[9]

In view, therefore, of the paucity of such information, we have launched synthetic efforts targeting soluble titanium complexes in the presence of citrate and hydrogen peroxide, with the metal ion being in the oxidation state +4. The relevant chemistry of titanium with hydrogen peroxide has been shown in the past to revolve around Ti−peroxy gels associated with reactive superoxide radical traps and interactions with other reactive species produced during inflammatory processes.[10] Hence, we report herein the synthesis, isolation from aqueous solutions, spectroscopic characterization, and structural determination of the first dinuclear titanium(IV)−peroxo−citrate complex. The possibilities and potential relevance of titanium(IV)−peroxo−citrate species to requisite biological interactions elicited by titanium are dwelled on.

Experimental Section

Materials and Methods. All experiments were carried out in the open air. Nanopure quality water was used for all reactions. $TiCl_4$, anhydrous citric acid, and H_2O_2 30% were purchased from Aldrich. Ammonia was supplied by Fluka.

Physical Measurements. FT-IR measurements were taken on a Perkin-Elmer 1760X FT-IR spectrometer. UV−vis spectra were recorded on a Hitachi U-2001 spectrophotometer in the range 200−900 nm. Elemental analyses were performed by Quantitative Technologies, Inc.

FT-Raman Spectroscopy. Fourier-transform-Raman (FT-Raman) measurements were obtained by using a Bruker (D) FRA-106/S component attached to an EQUINOX 55 spectrometer. An R510 diode pumped Nd:YAG polarized laser at 1064 nm (with a maximum output power of 500 mW) was used for Raman excitation in a 180° scattering sample illumination mode. Optical filtration reduced the Rayleigh elastic scattering and in combination with a CaF_2 beam splitter as well as a high sensitivity liquid N_2 cooled Ge-detector allowed Raman intensities to be recorded from 50 to 3300 cm^{-1} in the Stokes-shifted Raman region, all in one spectrum. The resulting spectra were an average of ∼350 scans, recorded at a resolution of 4 cm^{-1}; the laser was focused on the sample with an output power of ∼300 mW.

Laser Raman Microscopy. The Raman system used was the T-64000 model from Jobin Yvon (ISA-Horiba group). Raman spectra were excited by a linearly polarized monochromatic radiation at 514.5 nm, produced by a Spectra Physics air-cooled Ar^+ laser (model 163-A42). Circularly polarized light was obtained by intercalating a quarter wave-plate ($\lambda/4$) to the laser beam. A proper interference filter rejected plasma lines. The excitation beam was directed toward the microscope and with the use of a beam splitter and a microscope objective (50×/0.55 Olympus) it was focused on the sample. Raman scattered radiation was collected in a backscattering geometry by the same microscope objective, and by passing through the beam splitter and a notch filter it was focused on the slit of a single monochromator. The dispersion and the detection were done by a 1800-grooves/mm grating and by a 2D CCD detector (operating at 140 K), respectively. The resolution capability was maintained at approximately 4 cm^{-1}.

Solid-State NMR. The high resolution solid-state ^{13}C magic angle spinning (MAS) NMR spectra were measured at 100.63 MHz, on a Bruker MSL400 NMR spectrometer, capable of high power ^1H-decoupling. The spinning rate used for $^1H-^{13}C$ cross polarization and magic angle spinning experiments was 5 kHz at ambient temperature (25 °C). Each solid-state spectrum was a result of the accumulation of 200 scans. The recycle delay used was 4 s, the 90° pulse was 5 μs, and the contact time was 1 ms. All solid-state spectra were referenced to adamantane, which showed two peaks at 26.5 and 37.6 ppm, respectively, and to the external reference of TMS.

(5) (a) Shimizu, H.; Habu, T.; Takada, Y.; Watanabe, K.; Okuno, O.; Okabe, T. *Biomaterials* **2002**, *23*, 2275−2281. (b) Moroni, A.; Faldini, C.; Rocca, M.; Stea, S.; Giannini, S. *J. Orthop. Trauma* **2002**, *16*, 257−263 (c) Oka, M. *J. Orthop. Sci.* **2001**, *6*, 448−456.

(6) (a) Schwartz, Z.; Lohmann, C. H.; Vocke, A. K.; Sylvia, V. L.; Cochran, D. L.; Dean, D. D.; Boyan, B. D. *J. Biomed. Mater. Res.* **2001**, *56*, 417−426. (b) Takei, H.; Pioletti, D. P.; Kwon, S. Y.; Sung, K.-L. P. *J. Biomed. Mater. Res.* **2000**, *52*, 382−387. (c) Wang, J. Y.; Tsukayama, D. T.; Wicklund, B. H.; Gustilo, R. B. *J. Biomed. Mater. Res.* **1996**, *32*, 655−661.

(7) Suzuki, R.; Frangos, J. A. *Clin. Orthop. Relat. Res.* **2000**, *372*, 280−289.

(8) (a) Martin, R. B. *Inorg. Biochem.* **1986**, *28*, 181−187. (b) Glusker, J. P. *Acc. Chem. Res.* **1980**, *13*, 345−352.

(9) Kakihana, M.; Tada, M.; Shiro, M.; Petrykin, V.; Osada, M.; Nakamura, Y. *Inorg. Chem.* **2001**, *40*, 891−894.

(10) (a) Tengvall, P.; Elwing, H.; Sjoqvist, L.; Lundstrom, I.; Bjursten, L. *Biomaterials* **1989**, *10*, 118−120. (b) Tengvall, P.; Lundstrom, I.; Sjoqvist, L.; Elwing, H.; Bjursten, L. *Biomaterials* **1989**, *10*, 166−175. (c) Tengvall, P.; Walivaara, B.; Westerling, J.; Lundstrom, I. *J. Colloid Interface Sci.* **1991**, *143*, 589−592.

Table 1. Summary of Crystal, Intensity Collection, and Refinement Data for $(NH_4)_4[Ti_2(O_2)_2(C_6H_4O_7)_2]\cdot 2H_2O$ (**1**)

formula	$C_{12}H_{28}N_4O_{20}Ti_2$
fw	644.16
T, K	298
wavelength	Mo Kα 0.71073
space group	$P2_1/n$
a (Å)	10.360(4)
b (Å)	10.226(4)
c (Å)	11.478(6)
β, deg	107.99(2)
V, (Å^3)	1156.6(9)
Z	2
D_{calcd}/D_{measd} (Mg m^{-3})	1.769/1.75
abs coeff (μ), mm^{-1}	0.789
range of h,k,l	$-12 \rightarrow 11$, $-12 \rightarrow 0$, $0 \rightarrow 13$
GOF on F^2	1.127
R indices[a]	$R = 0.0287$, $R_w = 0.0785$[b]

[a] R values are based on F values; R_w values are based on F^2. $R = [\sum||F_o| - |F_c||]/[\sum(|F_o|)]$. $R_w = \{\sum[w(F_o^2 - F_c^2)^2]/\sum[w(F_o^2)^2]\}^{1/2}$. [b] For 1995 reflections with $I > 2\sigma(I)$.

Solution NMR. The samples for solution NMR studies were prepared by dissolving the crystalline complexes in D_2O, at concentrations in the range 0.02−0.10 M. NMR spectra were recorded on a Bruker AM360 (^{13}C) spectrometer. Chemical shifts (δ) are reported in ppm relative to an internal reference of TMS.

Preparation of Complex $(NH_4)_4[Ti_2(O_2)_2(C_6H_4O_7)_2]\cdot 2H_2O$ (1). A quantity of anhydrous citric acid (0.20 g, 1.0 mmol) was placed in a flask and dissolved in 2 mL of H_2O. Subsequently, $TiCl_4$ (0.20 g, 1.0 mmol) was added slowly and under continuous stirring. The resulting reaction mixture was allowed to stir overnight at room temperature. On the following day, the solution was colorless, and the pH was ∼1. Aqueous ammonia was added slowly to adjust the pH to a final value of ∼4.5. The reaction mixture was then placed in an ice bath. Under exclusion of light, an aqueous solution of hydrogen peroxide 30% (0.33 g, 9.7 mmol) was added slowly and under continuous stirring. The solution turned red and stayed as such. Stirring continued for an additional 15 min. Addition of cold ethanol at 4 °C resulted after several days in the deposition of a deep red crystalline material. The product was isolated by filtration and dried in vacuo. Yield: 0.26 g (∼74%). Anal. Calcd for **1**, $(NH_4)_4[Ti_2(O_2)_2(C_6H_4O_7)_2]\cdot 2H_2O$ ($C_{12}H_{28}N_4O_{20}Ti_2$, MW = 644.16): C, 22.35; H, 43.47; N, 8.69. Found: C, 22.13; H, 43.60; N, 8.61.

X-ray Crystallography. Crystal Structure Determination. X-ray quality crystals of compound **1** were grown from water−ethanol mixtures. A single crystal, with dimensions 0.15 × 0.40 × 0.44 mm^3 (**1**), was mounted on a Crystal Logic dual-goniometer diffractometer, using graphite monochromated Mo Kα radiation. Unit cell dimensions for **1** were determined and refined by using the angular settings of 25 automatically centered reflections in the range $11° < 2\theta < 23°$. Crystallographic details are given in Table 1. Intensity data were measured by using $\theta-2\theta$ scans. Three standard reflections were monitored every 97 reflections, over the course of data collection. They showed less than 3% variation and no decay. Lorentz and polarization corrections were applied by using Crystal Logic software. Further experimental crystallographic details for **1** follow: $2\theta_{max} = 51°$, scan speed 3.0°/min; scan range $2.3 + \alpha_1\alpha_2$ separation; reflections collected/unique/used, 2269/2159-(R_{int} = 0.0219)/2159; 228 parameters refined; $(\Delta/\sigma)_{max} = 0.006$; $(\Delta\rho)_{max}/(\Delta\rho)_{min} = 0.292/-0.463$ e/Å^3; R/R_w (for all data), 0.0318/0.0806.

The structure of complex **1** was solved by direct methods using SHELXS-86.[11] Refinement was achieved by full-matrix least-squares techniques on F^2 with SHELXL-93.[12] All non-H atoms in the structure of **1** were refined anisotropically. All H-atoms were located by difference maps and were refined isotropically. Two water solvate molecules were found to be present in the lattice of **1**.

Results

Synthesis. The synthesis of complex **1** was achieved by a simple procedure employing titanium tetrachloride and citric acid in water. Addition of aqueous ammonia raised the pH of the solution to ∼4.5, and concurrently provided the necessary counterions for the subsequently derived anionic complex. To the colorless reaction mixture arising from the above reagents, a solution of hydrogen peroxide H_2O_2 30% was added in sufficient excess to ensure the availability of the peroxo group for coordination to the titanium metal. The resulting red solution containing the peroxo product was treated with ethanol at 4 °C and afforded efficiently a red crystalline material.

The overall stoichiometric reaction leading to complex **1** is shown schematically.

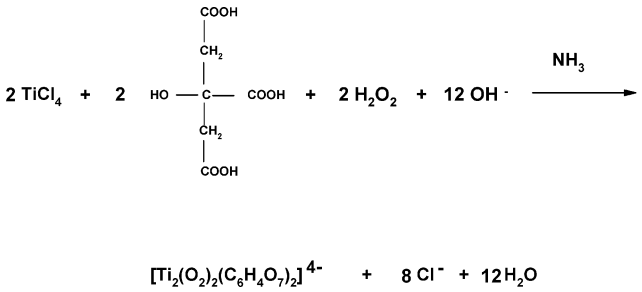

Elemental analysis on the isolated crystalline material suggested the formulation $(NH_4)_4[Ti_2(O_2)_2(C_6H_4O_7)_2]\cdot 2H_2O$ (**1**). Complex **1** in the crystalline form appears to be stable for long periods of time. It is insoluble in alcohols (CH_3OH, C_2H_5OH, and 2-PrOH), acetonitrile, and dimethyl sulfoxide (DMSO), but it dissolves readily in water.

Description of the Crystal Structure of $(NH_4)_4[Ti_2(O_2)_2(C_6H_4O_7)_2]\cdot 2H_2O$ (1). The X-ray crystal structure of **1** consists of discrete anions and ammonium cations. Complex **1** crystallizes in the monoclinic space group $P2_1/n$ with two molecules per unit cell. The ORTEP diagram of the anion in **1** is shown in Figure 1. A select list of interatomic distances and bond angles for **1** is given in Table 2. The anionic complex in **1** is a dimer of two titanium(IV) ions coordinated by two citrate ligands. Each citrate spans both Ti(IV) ions. The central core in the dimer is composed of a $Ti^{IV}_2O_2$ rhombic unit, which is planar by virtue of a center of inversion. The oxygens of the core unit originate in the alkoxides of the two citrate ligands coordinated around the two Ti(IV) ions. The two citrates are fully deprotonated. As

(11) Sheldrick, G. M S*HELXS-86: Structure Solving Program*; University of Göttingen: Göttingen, Germany, 1986.
(12) Sheldrick, G. M *SHELXL-93: Structure Refinement Program*; University of Göttingen: Göttingen, Germany, 1993.

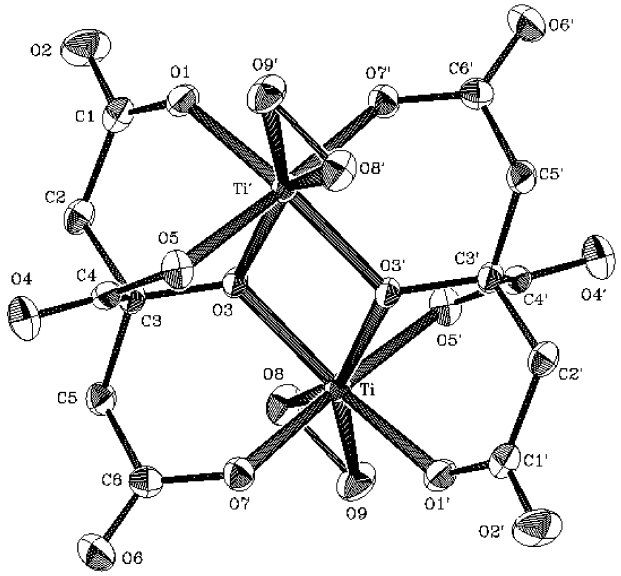

Figure 1. ORTEP structure of the $[Ti_2(O_2)_2(C_6H_4O_7)_2]^{4-}$ anion with the atom labeling scheme in **1**. Thermal ellipsoids are drawn by ORTEP and represent 50% probability surfaces.

Table 2. Bond Lengths [Å] and Angles [deg] in **1**[a]

Ti−O(8)	1.852(2)	Ti−O(1′)	2.069(2)
Ti−O(9)	1.890(2)	Ti−O(3′)	2.085(2)
Ti−O(3)	2.023(1)	Ti−O(5′)	2.049(2)
Ti−O(7)	2.026(2)		
O(8)−Ti−O(9)	45.97(7)	O(9)−Ti−O(1′)	82.08(6)
O(8)−Ti−O(3)	87.15(7)	O(3)−Ti−O(1′)	143.59(6)
O(9)−Ti−O(3)	132.42(6)	O(7)−Ti−O(1′)	83.97(6)
O(8)−Ti−O(7)	95.71(7)	O(5′)−Ti−O(1′)	92.08(6)
O(9)−Ti−O(7)	92.49(7)	O(8)−Ti−O(3′)	148.70(6)
O(3)−Ti−O(7)	83.32(6)	O(9)−Ti−O(3′)	153.31(6)
O(8)−Ti−O(5′)	86.82(7)	O(3)−Ti−O(3′)	71.36(6)
O(9)−Ti−O(5′)	87.09(7)	O(7)−Ti−O(3′)	103.80(6)
O(3)−Ti−O(5′)	99.87(6)	O(5′)−Ti−O(3′)	75.21(6)
O(7)−Ti−O(5′)	176.05(6)	O(1′)−Ti−O(3′)	78.83(5)
O(8)−Ti−O(1′)	128.05(6)	Ti−O(3)−Ti′	108.64(6)

[a] Symmetry transformations used to generate equivalent atoms: ′ $-x$, $-y$, $-z+1$.

such, they use all four available binding sites to anchor onto the Ti(IV) ions.

The coordination sphere around both Ti(IV) ions is completed with peroxo groups, one on each Ti(IV) center. The peroxide group O_2^{2-} binds to Ti(IV) in a side-on η^2-fashion, occupying two coordination sites in the equatorial plane, with the remaining three sites being taken by one terminal carboxylate group oxygen (O1′) from one citrate and the two central alkoxide groups (O3, O3′) from both coordinated citrate ligands. The apical positions in the bipyramid are occupied by the central carboxylate oxygen (O5′) of one citrate and the terminal carboxylate oxygen (O7) of the second citrate ligand. Ultimately, the coordination number around each Ti(IV) ion is seven, reflecting a pentagonal bipyramidal coordination environment for each metal center.

The Ti−O bond distances in **1** are in line with those in other Ti(IV) oxygen containing complexes, like $Na_4[Ti_2O_5(C_6H_6O_6N)_2]\cdot 11H_2O$ (**2**) (1.819(2)−2.065(2) Å),[13] $K_2[Ti_2O_5(C_7H_3O_4N)_2]\cdot 5H_2O$ (**3**) (1.825(2)−2.183(7) Å),[14] $(NH_4)_8[Ti_4(C_6H_4O_7)_4(O_2)_4]\cdot 8H_2O$ (**4**) (1.863(1)−2.085(1) Å),[9] and $Ti(O_2)(C_6H_4NO_2)_2\cdot OPN_3C_6H_{18}$ (**5**) (1.842(4)-2.042(4) Å).[15] It appears that similar angles are observed in **1** and a number of $Ti^{IV}(O_2)$ containing complexes, exhibiting pentagonal bipyramidal geometry around the titanium(IV) ions. Among such complexes are **3** (45.2(4)−100.8(4)°), **5** (45.2(2)−102.8(2)°), and $TiO_2(C_7H_3O_4N)(H_2O)_2\cdot 2H_2O$ (46.72(6)−95.73(6)°).[16]

Table 3. Hydrogen bonds in **1**

interaction	D···A (Å)	H···A (Å)	D−H···A (deg)	symmetry operation
Ow−Hwa···O2	2.887	2.096	170.6	$-x, -y, 1-z$
Ow−Hwb···O7	2.844	2.025	167.7	$1-x, -y, 1-z$
N1−HN1a··· O9	3.006	2.164	156.9	$-x, 1-y, 1-z$
N1−HN1b···O6	2.853	2.019	156.0	$-0.5+x, 0.5-y, 0.5+z$
N1−HN1c···O4	2.898	2.082	152.9	$-0.5-x, 0.5+y, 0.5-z$
N1−HN1d···O5	3.039	2.236	166.2	$-x, -y, 1-z$
N2−HN2a···O1	2.808	1.935	176.0	$-x, -y, 1-z$
N2−HN2b···Ow	2.895	2.085	168.1	$0.5+x, 0.5-y, 0.5+z$
N2−HN2c···O6	3.023	2.298	142.4	$0.5+x, 0.5-y, 0.5+z$
N2−HN2d···O2	3.114	2.313	149.3	$1+x, y, z$

The citrate ligands in the anion of **1** adopt an extended conformation upon binding to the titanium ion. The carbon atoms C(1), C(2), C(3), C(5), and C(6) of the citrate backbone are coplanar, with the largest standard deviation being 0.086 Å for C(2). The central carboxylate plane O(4)−C(4)−O(5) is rotated ∼8° out of the O(3)−C(3)−C(4) plane. These values are congruent with those seen in congener vanadium(V)−peroxo−citrate complexes, suggesting a similar approach of the citrate to the metal ions in the anionic assembly.[17]

The Ti···Ti distance in the anion of **1** is 3.336(1) Å, similar to those observed in the previously reported titanium(IV)−peroxo−carboxylate compound.[9]

Four ammonium counterions and two water molecules of crystallization per dinuclear anion are also present in the lattice of **1**. The ammonium cations and the water solvent molecules are in contact with the carboxylate oxygens of the citrate ligands and the peroxo oxygens, establishing an extensive hydrogen-bonding network (Table 3) responsible for the stability of the crystal lattice in **1**.

UV−Vis Spectroscopy. The electronic spectra of **1** were recorded in H_2O at pH ∼ 4 (Figure 2). The spectrum showed a band at 356 nm ($\epsilon = 3032$) with a rising absorbance into the ultraviolet region leading to a strong band at 207 nm ($\epsilon = 21\,129$). The spectrum was featureless beyond 500 nm. Given that Ti(IV) has no d electrons, attention was focused on the band close to the ultraviolet region.[18] The presence of the weaker feature at 356 nm could be reasonably

(13) Schwarzenbach, D.; Girgis, K. *Helv. Chim. Acta* **1975**, *58*, 2391−2398.
(14) Schwarzenbach, D. *Inorg. Chem.* **1970**, *9*, 2391−2397.
(15) Mimoun, H.; Postel, M.; Casabianca, F.; Fischer, J.; Mitschler, A. *Inorg. Chem.* **1982**, *21*, 1303−1306.
(16) Schwarzenbach, D. *Helv. Chim. Acta* **1972**, *55*, 2990−3004.
(17) Tsaramyrsi, M.; Kavousanaki, D.; Raptopoulou, C. P.; Terzis, A.; Salifoglou, A. *Inorg. Chim. Acta* **2001**, *320*, 47−59.
(18) (a) Ceccato, A. S.; Neves, A.; de Brito, M. A.; Drechsel, S. M.; Mangrich, A. S.; Werner, R.; Haase, W.; Bortoluzzi, A. J. *J. Chem. Soc., Dalton Trans.* **2000**, 1573−1577. (b) Robbins, D. J.; Stillman, M. J.; Thomson, A. J. *J. Chem. Soc., Dalton Trans.* **1974**, 813−820. (c) Syamal, A.; Theriot, L. J. *J. Coord. Chem.* **1973**, *2*, 193−200. (d) Lee, C. C.; Syamal, A.; Theriot, L. J. *Inorg. Chem.* **1971**, *10*, 1669−1673. (e) Sacconi, L.; Campigli, U. *Inorg. Chem.* **1966**, *5*, 606−611.

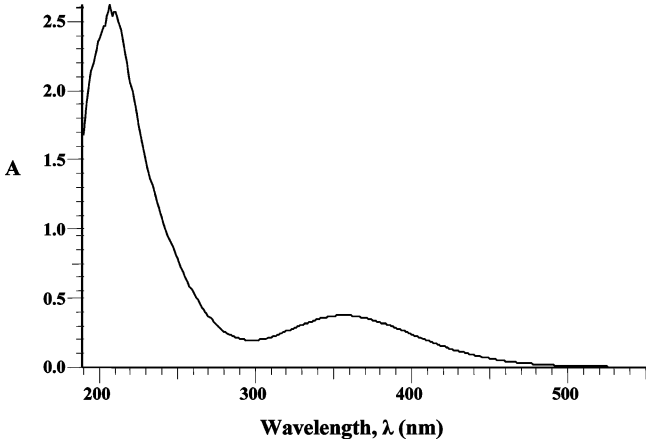

Figure 2. Electronic spectrum of $(NH_4)_4[Ti_2(O_2)_2(C_6H_4O_7)_2]\cdot 2H_2O$ (**1**) in water.

attributed to a $\pi_v^* \rightarrow$ d ligand to metal charge transfer (LMCT) band. The intense absorption feature at 207 nm could be associated with the $\pi_h^* \rightarrow d\sigma^*$ LMCT transition. The latter was proposed to appear at energies higher than the $\pi_v^* \rightarrow$ d transition, owing to the stabilization of the π_h^* peroxo to Ti(IV) ligand to metal σ-bonding orbital, in line with past reports in the literature.[19]

FT-IR Spectroscopy. The FT-IR spectrum of **1** in KBr revealed the presence of vibrationally active carboxylate groups. Antisymmetric as well as symmetric vibrations for the carboxylate groups of the coordinated citrate ligands dominated the spectrum. Specifically, antisymmetric stretching vibrations $\nu_{as}(COO^-)$ were present for the carboxylate carbonyls in the range 1630−1592 cm^{-1}. Symmetric vibrations $\nu_s(COO^-)$ for the same groups were present in the range 1445−1335 cm^{-1}. The frequencies of the observed carbonyl vibrations were shifted to lower values in comparison to the corresponding vibrations in free citric acid, indicating changes in the vibrational status of the citrate ligand upon coordination to the titanium ion.[20] The difference between the symmetric and antisymmetric stretches, $\Delta(\nu_{as}(COO^-) - \nu_s(COO^-))$, was greater than 200 cm^{-1}, indicating that the carboxylate groups of the citrate ligand were either free or coordinated to the metal ion in a monodentate fashion.[20,21] This was further confirmed by the X-ray crystal structure of **1**. The O−O vibration of the peroxo groups in **1** was present around 876 cm^{-1}. There is also a band around 606 cm^{-1}, which has been attributed to the presence of $\nu_s(Ti-(O_2))$ vibrations. The corresponding frequency for the $\nu_{as}(Ti-(O_2))$ vibrations was observed around 525 cm^{-1}.[19d] All of the aforementioned assignments were in agreement with previous assignments in dinuclear Ti(IV)−peroxo complexes,[22,9] and in line with prior reports on peroxo and non-peroxo carboxylate containing ligands bound to different metal ions.[17,23−26]

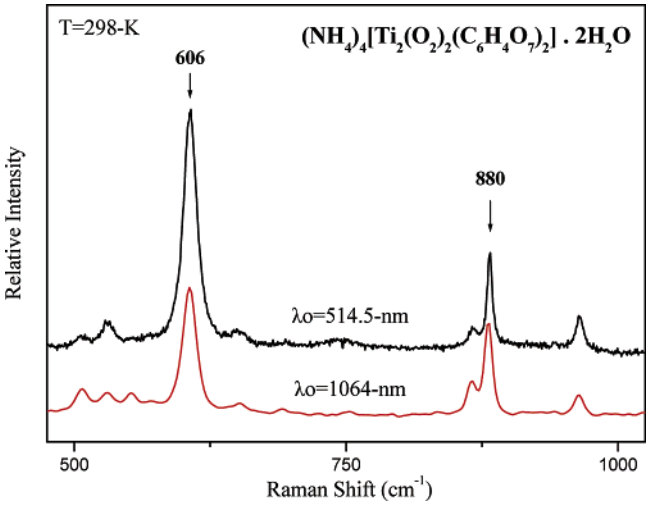

Figure 3. Top: Raman spectrum of $(NH_4)_4[Ti_2(O_2)_2(C_6H_4O_7)_2]\cdot 2H_2O$ (**1**) in the solid state. Excitation with a visible laser line at 514.5 nm. Bottom: FT-Raman spectrum of **1** with a near-IR excitation at 1064 nm.

Raman Spectroscopy. Raman spectroscopy has been employed to provide structural details in **1**. This spectroscopic method has been used extensively to report the presence of coordinated peroxide species, since bridged dioxygen complexes could be readily identified in their Raman spectra due to the presence of the well-characterized O−O stretch.[27] In Figure 3 (top), the Raman spectrum of complex **1** in the solid state, excited with a visible laser line, is shown in the spectral window of stretching modes for metal-coordinated peroxo species. In order to avoid polarization preferences of the vibrational normal modes, depending on the crystal orientation versus the laboratory coordinates, the excitation laser light was circularly polarized. The more intense Raman scattering peaks located at 606 and 880 cm^{-1} are attributed to the $Ti-O_2$ and O−O symmetric stretching vibrations, respectively, in accordance with the characteristic spectral features reported in the literature for a peroxo−metal compound, with the peroxide group bound to the Ti metal center in a side-on fashion.[28−30] The weak Raman peak at ∼530 cm^{-1} might tentatively be attributed to the $Ti-O_2$ antisymmetric stretch. A similar energy ordering of $\nu_s(M-O)$ and

(19) (a) Lever, A. B. P. In *Inorganic Electronic Spectroscopy*, 2nd ed.; Elsevier: Amsterdam, 1984. (b) Lever, A. B. P.; Ozin, G. A.; Gray, H. B. *Inorg. Chem.* **1980**, *19*, 1823−1824. (c) Lever, A. B. P.; Gray, H. B. *Acc. Chem. Res.* **1978**, *11*, 348. (d) Jeske, P.; Haselhorst, G.; Weyhermüller, T.; Wieghardt, K.; Nuber, B. *Inorg. Chem.* **1994**, *33*, 2462−2471.
(20) Deacon, G. B.; Philips, R. *J. Coord. Chem. Rev.* **1980**, *33*, 227−250.
(21) Djordjevic, C.; Lee, M.; Sinn, E. *Inorg. Chem.* **1989**, *28*, 719−723.
(22) Nakamoto, K. In *Infrared and Raman Spectra of Inorganic and Coordination Compounds, Part B*, 5th ed.; John Wiley and Sons: New York, 1997.
(23) (a) Matzapetakis, M.; Raptopoulou, C. P.; Terzis, A.; Lakatos, A.; Kiss, T.; Salifoglou, A. *Inorg. Chem.* **1999**, *38*, 618−619. (b) Matzapetakis, M.; Raptopoulou, C. P.; Tsohos, A.; Papefthymiou, B.; Moon, N.; Salifoglou, A. *J. Am. Chem. Soc.* **1998**, *120*, 13266−13267. (c) Matzapetakis, M.; Dakanali, M.; Raptopoulou, C. P.; Tangoulis, V.; Terzis, A.; Moon, N.; Giapintzakis, J.; Salifoglou, A. *JBIC, J. Biol. Inorg. Chem.* **2000**, *5*, 469−474. (d) Matzapetakis, M.; Karligiano, N.; Bino, A.; Dakanali, M.; Raptopoulou, C. P.; Tangoulis, V.; Terzis, A.; Giapintzakis, J.; Salifoglou, A. *Inorg. Chem.* **2000**, *39*, 4044−4051.
(24) Griffith, W. P.; Wickins, T. D. *J. Chem. Soc. A* **1968**, 397−400.
(25) Vuletic, N.; Djordjevic, C. *J. Chem. Soc., Dalton Trans.* **1973**, 1137−1141.
(26) Kaliva, M.; Giannadaki, T.; Raptopoulou, C. P.; Tangoulis, V.; Terzis, A.; Salifoglou, A. *Inorg. Chem.* **2001**, *40*, 3711−3718.
(27) Vacque, V.; Sombret, B.; Huvenne, J. P.; Legrand, P.; Suc, S. *Spectrochim. Acta, Part A* **1997**, *53*, 55−66.
(28) Griffith W. P. *J. Chem. Soc.* **1964**, 5248−5552.
(29) Chaudhuri, M. K.; Das, B. *Inorg. Chem.* **1986**, *25*, 168−170.
(30) Nour, E. M.; Morsy, S. *Inorg. Chim. Acta* **1986**, *117*, 45−48.

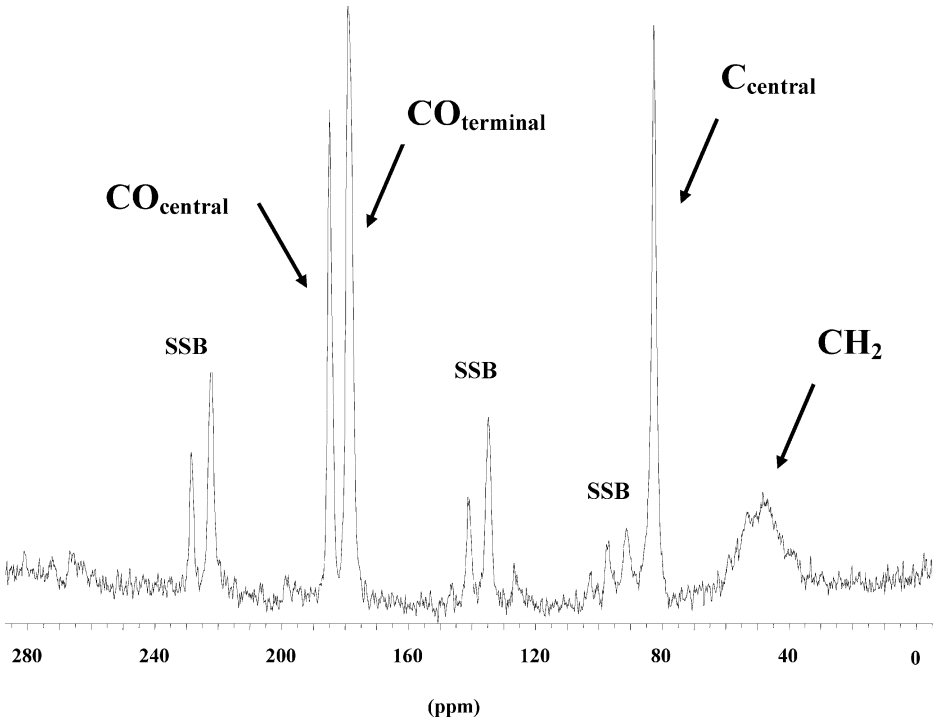

Figure 4. ^{13}C MAS NMR spectrum of $(NH_4)_4[Ti_2(O_2)_2(C_6H_4O_7)_2]\cdot 2H_2O$ (**1**) in the solid state. SSB signifies the presence of spinning sidebands.

$\nu_{as}(M-O)$ vibrations has been previously observed[31] in an end-on peroxide-bridged coupled binuclear copper(II) complex (M = Cu), for which normal-coordinate analysis reveals the importance of the metal−peroxide bending mode value that influences the magnitudes of the M−O force constant. In close proximity to the O−O symmetric stretch, there exists another weak spectral feature, located at 866 cm^{-1}, that cannot be easily assigned. Most likely, it originates from a splitting of the ν_{O-O} normal mode. A similar splitting for the O−O peroxide stretch has been previously attributed either to the in-phase−out-of-phase vibration of two metal-coordinated peroxo groups in ammonium difluorodiperoxytitanates(IV)[29] or to a correlation splitting between metal-coordinated O_2^{2-} groups in different site symmetries for sodium peroxide.[27] The prevailing reason for the ν_{O-O} splitting in **1**, if any, may be linked to the presence of the NH_4^+ and H_2O mediating molecules in the lattice that could introduce some type of differential mechanical coupling effect in this side-on bound peroxide. Moreover, the Raman peak at 606 cm^{-1} exhibits a pre-resonance-Raman effect, since the excitation laser line at 514.5 nm resides on the tail of the $O_2^{2-} \rightarrow$ Ti(IV) charge transfer transition type of absorption band for **1** at 356 nm. This is confirmed by relevant FT-Raman spectra with near-IR excitation, where the Raman peaks at 606 and 880 cm^{-1} exhibit comparable scattering intensities (bottom of Figure 3). The different behavior of these two bands toward resonance enhancement may be due to an excited-state distortion of the charge transfer excitation, depending on the extent of electron delocalization.

Solid-State NMR Spectroscopy. The MAS ^{13}C NMR spectrum of **1** (Figure 4) is consistent with the coordination mode of citrate around the Ti(IV) ion. The spectrum showed four separate peak features. Two of those lie in the high field region whereas the other two appear in the low field region. The broad peak(s) in the high field region could be assigned to the two methylene carbons (48.1 ppm) located adjacent to the coordinated terminal carboxylates of the citrate ligand. The resonance at 82.6 ppm is reasonably attributed to the central carbon atom located adjacent to the bound central carboxylate group. In the low field region, where the carbonyl carbon resonances are expected, there was only one peak observed (179.0 ppm) for the terminal carboxylate groups, both bound to the two Ti(IV) ions of the central core. There is also one peak observed (184.9 ppm) for the bound central carboxylate carbon of the citrate ligand. This signal is shifted to lower field by 5.9 ppm in comparison to the previous signal for the terminal carboxylate groups, most likely due to the presence of the nearby ionized alkoxide group. A similar pattern of ^{13}C resonances was observed in the case of mononuclear complexes, such as $(NH_4)_5[Al(C_6H_4O_7)_2]\cdot 2H_2O$,[32] the tetranuclear complex $(NH_4)_8[Ti_4(C_6H_4O_7)_4(O_2)_4]\cdot 8H_2O$ (**4**),[9] and dinuclear complexes such as $Na_2[Bi_2(C_6H_4O_7)_2]\cdot 7H_2O$.[33] In the latter case, fully resolved resonances were observed for the carbons of the two variably bound CH_2COO^- groups (one is bound in a bidentate fashion to the bismuth ion, whereas the other one serves as a bridge to two bismuth ions).

Solution NMR Spectroscopy. The solution ^{13}C NMR spectrum of complex **1** was recorded in D_2O. The spectrum

(31) Baldwin, M. J.; Ross, P. K.; Pate, J. E.; Tyeklár, Z.; Karlin, K. D.; Solomon, E. I. *J. Am. Chem. Soc.* **1991**, *113*, 8671−8679.

(32) Matzapetakis, M.; Kourgiantakis, M.; Dakanali, M.; Raptopoulou, C. P.; Terzis, A.; Lakatos, A.; Kiss, T.; Banyai, I.; Iordanidis, L.; Mavromoustakos, T.; Salifoglou, A. *Inorg. Chem.* **2001**, *40*, 1734−1744.

(33) Barrie, P. J.; Djuran, M. I.; Mazid, M A.; McPartlin, M.; Sadler, P. J.; Scowen, I. J.; Sun, H. *J. Chem. Soc., Dalton Trans.* **1996**, 2417−2422.

showed six peaks. The two peaks appearing in the high field region (46.5 and 46.9 ppm) were assigned to the CH_2 groups of the bound citrate ligand spanning the two Ti(IV) ions. The resonance at 86.4 ppm was attributed to the central carbon of the bound citrate. The two signals at 180.7 and 181.4 ppm in the lower field region were assigned to the terminal carboxylate carbons attached to the two Ti(IV) ions. The signal located at the low end of the field (187.4 ppm) was assigned to the central carboxylate carbon attached to the Ti(IV) ion. This signal was significantly shifted to lower fields in comparison to the other two signals belonging to the terminal carboxylate carbons. The shift was ~7.0 ppm downfield and was comparable to that observed in the MAS ^{13}C solid-state spectrum of **1**. Here as well, the shift was likely due to the proximity of the central carboxylate carbon to the ionized alkoxide group of the Ti(IV) coordinated citrate. Overall, the pattern of resonances observed was similar to that observed in the solid-state ^{13}C-MAS NMR spectrum of **1**, showing consistency between the solid and solution states. The time dependent NMR spectra of **1** in water, over a period of 24 h, showed no significant changes in the type of resonance and frequency at which the aforementioned resonances appear. That signified the stability of the species in solution. Collectively, the data support the picture of the dinuclear complex provided by the solid-state NMR spectrum of **1**. Further work on the potential NMR dinuclear structure(s) in solution is expected to shed light on the specific structural attributes of the citrates coordinated to $Ti_2^{IV}O_2$ cores. Such work is currently in progress.

Discussion

Chemical, Structural, and Spectroscopic Considerations of the d^0 Metal Ion Ti(IV). Synthetic efforts on the aqueous ternary system Ti(IV)−H_2O_2−citric acid have led to the isolation of the first dinuclear Ti−peroxo−citrate complex $(NH_4)_4[Ti_2(O_2)_2(C_6H_4O_7)_2]\cdot 2H_2O$ (**1**). Key to this success was the expedient reactivity of the admittedly complex reaction system, which in a pH specific fashion afforded the requisite complex. Essential in unraveling the chemical and physical properties of this aqueous species was the employment of a plethora of analytical and spectroscopic techniques (FT-IR, Raman, UV−vis, ^{13}C-MAS NMR, and solution ^{13}C NMR spectroscopy) supplemented by X-ray crystallography. Hence, from the presence of the Ti(IV)−(O_2) moiety to the citrate mode of coordination and the consequent configuration of the pentagonal bipyramidal coordination, the structural and spectroscopic data reflected consistently the presence of **1** as a discrete species.

From the Ti(IV)−citrate chemistry point of view, the only cognate molecule with which complex **1** relates directly is complex $(NH_4)_8[Ti_4(C_6H_4O_7)_4(O_2)_4]\cdot 8H_2O$ (**4**).[9] Complex **4** is a tetranuclear species, composed of two dinuclear units, which appear to be similar to that in complex **1**. In each dinuclear unit, there exists one $[Ti_2O_2(O_2)_2]^{2+}$ core, to which two citrate ligands are bound. Both citrate ligands are fully deprotonated. There are two terminal carboxylates on each unit, one per citrate, which do not participate in coordination to the Ti(IV) core of their unit. One of these carboxylates serves as a bridge between the two structural units in the overall complex, coordinating to the core of the adjacently located dinuclear assembly in a bidentate fashion and spanning both Ti(IV) centers of the core. Thus, there are two terminal carboxylate bridges in the tetranuclear assembly. Consequently, the basic structural characteristics encountered in **1** are also seen in **4**, including (a) the deprotonation state of the citrate ligands in both species, (b) the use of the central carboxylate and alkoxide moieties and one of the terminal carboxylates for coordination to the Ti(IV) core(s), (c) the coordination number and geometry around each Ti(IV) ion of the core(s), and (d) the peroxide group O_2^{2-} in both species lying in the equatorial plane of the $Ti^{IV}{}_2O_2$ core. Striking differences between the two species include the following: (a) All potential coordination sites of the two citrate ligands are used to bind to the core in **1** but not in **4**, where one of the terminal carboxylates abstains from binding to the core whereas the other one serves as a bridge to bind to the adjacent assembly, thus giving rise to the tetranuclear complex. (b) Each carboxylate of the citrate ligand in **1** binds to the $Ti^{IV}{}_2O_2$ core in a monodentate fashion in contrast to the citrate ligands in **4**, where one of the terminal carboxylates binds to the adjacent $Ti^{IV}{}_2O_2$ core in a bidentate fashion.

In view of the aforementioned structural account of the Ti(IV)−peroxo−citrate assemblies, it appears that the elaborated on structural attributes are quite familiar features in the metal ion citrate aqueous chemistry. Actually, it appears that the synthetic chemistry between the early transition metal ion Ti(IV) and physiological ligands, like citric acid, offers a number of parallelisms with similar chemistries unfolding between citric acid, H_2O_2, and vanadium(V). Vanadium is the element adjacent to titanium in the periodic table, with the same metal ion electronic configuration (Ti(IV) vs V(V)). Therefore, its chemistry with citric acid may be similar to the corresponding titanium chemistry in a number of different respects. As a matter of fact, comparison of the structure of the dinuclear complex **1** with the spectroscopically and structurally characterized dinuclear complex $(NH_4)_6[V_2O_2(O_2)_2(C_6H_4O_7)_2]\cdot 4.5H_2O$ (**6**)[34] leads to a number of interesting observations.

Similarities between the two species include the following: (1) In complex **1**, Ti(IV) has an electronic configuration d^0. The same electronic configuration is possessed by V(V) (d^0) in $(NH_4)_6[V_2O_2(O_2)_2(C_6H_4O_7)_2]\cdot 4.5H_2O$. (2) In both complexes, the citrate ligands are fully deprotonated. (3) In both complexes, the basic mode of citrate coordination is the same. The citrates utilize as a minimum number of anchoring metal sites the central alkoxide and carboxylate groups. The only other complex of vanadium, where both citrates are fully deprotonated and all binding sites are used to coordinate to the vanadium ions, is $(NH_4)_4[V^{IV}{}_2O_2(C_6H_4O_7)_2]\cdot 2H_2O$.[35] (4) As a result of the citrate coordination mode to Ti(IV) and V(V) in **1** and **6**, respectively, the planar $Ti^{IV}{}_2O_2$ and $V^{V}{}_2O_2$ rhombic cores, which serve as the scaffold

(34) Kaliva, M.; Raptopoulou, C. P.; Terzis, A.; Salifoglou, A. Submitted for publication.

of the anionic assemblies, configure structural entities with the same coordination number seven. (5) The coordination geometry around Ti(IV) and V(V) in **1** and **6**, respectively, is a pentagonal bipyramid. (6) Both complexes are dinuclear. (7) Both complexes are anionic, with a total charge ≥ 4.

The major differences observed between the two structures include the following: (1) The charge of the anionic complex **1** is 4−, whereas that of complex **6** is 6−. (2) In the case of complex **1**, all four binding sites of the citrate ligands are used to coordinate to Ti(IV). In the case of complex **6**, the two terminal carboxylate groups, albeit deprotonated, do not both participate in coordination to the two vanadium(V) ions.

Links to Ti(IV)−Peroxo−Citrate Speciation. Projection to Potential Role(s) of Ti(IV) in Biological Fluids. The importance of complex **1** is tightly linked to Ti(IV)−peroxo−citrate speciation in aqueous media. Such a study, however, is not presently available. It would certainly formulate a comprehensive view of the Ti(IV) species, in the presence of citric acid and hydrogen peroxide, as a function not only of pH but also of concentration of the involved partners in aqueous media. Moreover, information relating to the Ti(IV)−peroxo−citrate as well as Ti(IV)−citrate speciation would help establish the basis of understanding the interactions of Ti(IV) with biologically relevant molecules.

Titanium has been increasingly involved in materials affecting the quality of life in humans.[36] In this sense, titanium is an essential component of prosthetics used in surgical rectification of human skeletal aberrations or a multitude of traumatic bone related problems. It is also used in dental fillings and in the form of powder particles in several other instances. Therefore, titanium in one form or another comes in contact with biological tissues. Consequently, it elicits interactions from biological fluids containing biological molecules of both low and high molecular mass. In so doing, it interacts with physiological target molecules of variable size and biological function. In all of such cases, the logical question arises as to what types of interactions develop between that element or ion (in its solubilized form(s)) and the adjoining biological tissue. To this end, the nature and extent of aqueous chemical interactions of titanium with physiological components is essential. Thus, the solubility and bioavailability of this metal ion in aqueous media acquires special significance, and due attention should be given.

Concomitantly, to the degree that bioavailable species of titanium with physiological ligands interact with cellular components or interdict biological pathways, valuable information is expected to arise from relevant synthetic endeavors, which will enable in-depth probing of biological interactions that avail themselves in a multitude of clinical symptoms, explicitly described in clinical investigations. Such investigations have largely proposed macroscopic roles for titanium (pure or in alloys and composites) involved in protein expression,[37] growth factor recruitment,[38] signal transduction,[39] enzyme activation,[40] gene expression,[41] and others.[42]

On the basis of the aforementioned grounds, the work presented here on complex **1** is the beginning of a research initiative aiming at understanding the chemical background of the interactions of titanium with physiological ligands in biologically relevant media. Studies in this direction are currently ongoing in our labs.

Acknowledgment. This work was supported with funds provided by the Department of Chemistry, University of Crete, Greece.

Supporting Information Available: X-ray crystal crystallographic files, in CIF format, and listings of positional and thermal parameters and H-bond distances and angles for **1**. This material is available free of charge via the Internet at http://pubs.acs.org.

IC0343051

(35) Tsaramyrsi, M.; Kaliva, M.; Giannadaki, T.; Raptopoulou, C. P.; Tangoulis, V.; Terzis, A.; Giapintzakis, J.; Salifoglou, A. *Inorg. Chem.* **2001**, *40*, 5772−5779.

(36) (a) Ortorp, A.; Jemt, T. *Clin. Implant Dent. Relat. Res.* **2002**, *4*, 104−109. (b) Kindberg, H.; Gunne, J.; Kronstrom, M. *Int. J. Prosthodont.* **2001**, *14*, 575−581. (c) Ravasi, F.; Sansone, V. *Arch. Orthop. Trauma Surg.* **2002**, *122*, 350−353.

(37) Bledsoe, J. G.; Slack, S. M. *J. Biomater. Sci., Polym. Ed.* **1998**, *9*, 1305−1312.

(38) Frenkel, S. R.; Simon, J.; Alexander, H.; Dennis, M.; Ricci, J. L. *J. Biomed. Mater. Res.* **2002**, *63*, 706−713.

(39) Vermes, C.; Roebuck, K. A.; Chandrasekaran, R.; Dobai, J. G.; Jacobs, J. J.; Glant, T. T. *J. Bone Miner. Res.* **2000**, *15*, 1756−1765.

(40) Palmbos, P. L.; Sytsma, M. J.; DeHeer, D. H.; Bonnema, J. D. *J. Orthop. Res.* **2002**, *20*, 483−489.

(41) (a) Kapanen, A.; Kinnunen, A.; Ryhanen, J.; Tuukkanen, J. *Biomaterials* **2002**, *23*, 3341−3346. (b) Kwon, S. Y.; Lin, T.; Takei, H.; Ma, Q.; Wood, D. J.; O'Connor, D.; Sung, K. L. *Biorheology* **2001**, *38*, 161−183.

(42) Guo, M.; Sun, H.; McArdle, H. J.; Gambling, L.; Sadler, P. J. *Biochemistry* **2000**, *39*, 10023−10033.